Scattered light fluorescence microscopy in three dimensions

Giulia Ghielmetti[1] **and Christof M. Aegerter**[1,*]

[1] *Physik-Institut, University of Zurich, Winterthurerstrasse 190, 8057 Zurich, Switzerland*

[*] *aegerter@physik.uzh.ch*

Abstract: Recently, we have proposed a method to image fluorescent structures behind turbid layers at diffraction limited resolution using wave-front shaping and the memory effect. However, this was limited to a raster scanning of the wave-front shaped focus to a two dimensional plane. In applications, it can however be of great importance to be able to scan a three dimensional volume. Here we show that this can be implemented in the same setup. This is achieved by the addition of a parabolic phase shift to the shaped wave-front. Via the memory effect, this phase shift leads to a shift of the interference based focus in the z-direction, thus opening the possibility of three dimensional imaging using scattered light fluorescence microscopy. Here, we show an example of such a three dimensional image of fluorescent nano-beads taken behind a turbid layer more than 10 mean free paths thick. Finally, we discuss the differences of the scanning in the z-direction with that in the x-y plane and the corresponding possibilities and limitations of the technique.

© 2012 Optical Society of America

OCIS codes: (290.4210) Multiple scattering; (110.0180) Microscopy; (110.7050) Turbid media; (030.6140) Speckle.

References and links

1. J. B. Pawley ed., *Handbook of Biological Confocal Microscopy,* 3rd ed. (Springer, Berlin 2006).
2. F. Helmchen and W. Denk, "Deep tissue two-photon microscopy," Nat. Methods **2**, 932–940 (2005).
3. A. Diaspro, ed., *Confocal and Two-Photon Microscopy: Foundations, Applications and Advances* (Wiley-Liss, New York, 2002).
4. C. Vinegoni, C. Pitsouli, D. Razansky, N. Perrimon, and V. Ntziachristos, "In vivo imaging of Drosophila melanogaster pupae with mesoscopic fluorescence tomography," Nat. Methods **5**, 45–47 (2008).
5. M. Wolf, M. Ferrari, and V. Quaresima, "Progress of near-infrared spectroscopy and topography for brain and muscle clinical applications," J. Biomed. Opt. **12**, 062104 (2007).
6. I. M. Vellekoop and A. P. Mosk, "Focusing coherent light through opaque strongly scattering media," Opt. Lett. **32**, 2309–2311 (2007).
7. I. M. Vellekoop and C. M. Aegerter, "Scattered light fluorescence microscopy: imaging through turbid media," Opt. Lett. **35**, 1245–1247 (2010).
8. C. L. Hsieh, Y. Pu, R. Grange, G. Laporte, and D. Psaltis, "Imaging through turbid layers by scanning the phase conjugated second harmonic radiation from a nanoparticle," Opt. Express **18**, 20723–20731 (2010).
9. M. Cui, E. J. McDowell, and C. Yang, "An in vivo study of turbidity suppression by optical phase conjugation (TSOPC) on rabbit ear," Opt. Express **18**, 25–30 (2010).
10. M. Cui and C. Yang, "Implementation of a digital optical phase conjugation system and its application to study the robustness of turbidity suppression by phase conjugation," Opt. Express **18**, 3444–3455 (2010).
11. G. Lerosey, J. de Rosny, A. Tourin, and M. Fink, "Focusing beyond the diffraction limit with far-field time reversal," Science **315**, 1120–1122 (2007).
12. Z. Yaqoob, D. Psaltis, M. S. Feld, and C. Yang, "Optical phase conjugation for turbidity suppression in biological samples," Nat. Photonics **2**, 110–115 (2008).

#159649 - $15.00 USD Received 7 Dec 2011; revised 23 Jan 2012; accepted 26 Jan 2012; published 31 Jan 2012
(C) 2012 OSA

13. M. Fink, "Time reversed acoustics," Phys. Today **50**, 34–40 (1997).
14. J. L. Thomas, F. Wu, and M. Fink, "Time reversal focusing applied to lithotripsy," Ultras. Imag. **18**, 106–121 (1996).
15. S. M. Popoff, G. Lerosey, R. Carminati, M. Fink, A. Boccara, and S. Gigan, "Measuring the transmission matrix in optics: an approach to the study and control of light propagation in disordered media," Phys. Rev. Lett. **104**, 100601 (2010).
16. S. M. Popoff, G. Lerosey, M. Fink, A. C. Boccara, and S. Gigan, "Image transmission through an opaque material," Nat. Commun. **1**, 81 (2010).
17. I. M. Vellekoop, A. Lagendijk, and A. P. Mosk, "Exploiting disorder for perfect focusing," Nat. Photonics **4**, 320–322 (2010).
18. Y. G. Ma, S. Sahebdivan, C. K. Ong, T. Tyc, and U. Leonhardt, "Evidence for subwavelength imaging with positive refraction," New J. Phys. **13**, 033016 (2011).
19. I. M. Vellekoop and A. P. Mosk, "Universal optimal transmission of light through disordered materials," Phys. Rev. Lett. **101**, 120601 (2008).
20. D. L. Fried, "Anisoplanatism in adaptive optics," J. Opt. Soc. Am. 72, 52–61 (1982).
21. S. Feng, C. Kane, P. A. Lee, and A. D. Stone, "Correlations and fluctuations of coherent wave transmission through disordered media," Phys. Rev. Lett. **61**, 834–837 (1988).
22. I. Freund, M. Rosenbluh, and S. Feng, "Memory effects in propagation of optical waves through disordered media," Phys. Rev. Lett. **61**, 2328–2331 (1988).
23. I. M. Vellekoop, E. G. van Putten, A. Lagendijk, and A. P. Mosk, "Demixing light paths inside disordered metamaterials," Opt. Express **16**, 67–80 (2008).
24. D. Akbulut, T. J. Huisman, E. G. van Putten, W. L. Vos, and A. P. Mosk, "Focusing light through random photonic media by binary amplitude modulation," Opt. Express **19**, 4017–4029 (2011).
25. D. B. Conkey, A. M. Caravaca-Aguirre, and R. Piestun, "High-speed scattering medium characterization with application to focusing light through turbid media," Opt. Express **20**, 1733–1740 (2012).
26. M. Cui, "A high speed wavefront determination method based on spatial frequency modulations for focusing light through random scattering media," Opt. Express 19, 2989–2995 (2011).
27. I. M. Vellekoop and C. M. Aegerter, "Focusing light through living tissue," Proc. SPIE **7554**, 755430 (2010).

1. Introduction

Imaging behind turbid structures is of great importance in applications of biomedical photonics, where often interesting structures are hidden behind turbid layers. Therefore, there have been many attempts to enable the imaging of such structures obscured by turbidity. One prominent way of circumventing this problem has been to discard scattered light with increasing efficiency, e.g. by using confocal microscopy [1] or two-photon microscopy [2]. Multi-photon microscopy has the advantage of using a spectral range of illuminating light where scattering in most biological tissues is less prominent [3]. One drawback is that due to the high photon densities needed to excite multi-photon processes, this needs pulsed laser sources on rather short time scales of tens of femtoseconds. In spite of these great advances, even in the best case of two-photon confocal microscopy, the penetration depth for useful imaging is limited to roughly 500 μm, which for many applications is insufficient [2]. An alternative route to the treatment of scattering in imaging applications is to compromise on the spatial resolution that can be obtained while increasing the penetration depth. This is for instance done in optical tomography [4], where using fluorescence contrast, structures deep within a tissue (up to 3 cm) [5] can be resolved, albeit at a reduced resolution of at most a few hundred microns [4, 5].

In a different field, there has recently been much activity in using the scattered light for imaging purposes, by controlling the spatial distribution of the phase of the incoming light [6–10]. These methods are based on the time-reversal symmetry of the scattering process [11]. This means that a phase conjugated, or temporally reversed field after scattering will make the inverted sequence of scattering, thus leading to a focus at the point of origin of the scattered wave [12]. This has first been intensely studied using sound waves [13], where a greater degree of control is available and where applications e.g. in the destruction of kidney stones are already in use clinically [14]. In the case of light, similar setups have been used to create a focused beam behind strongly scattering materials. This has been done in different ways. At a first instance, an

#159649 - $15.00 USD Received 7 Dec 2011; revised 23 Jan 2012; accepted 26 Jan 2012; published 31 Jan 2012
(C) 2012 OSA

iterative scheme was used where every pixel in a spatial light modulator is adjusted individually, thus leading to a global minimum [6]. Subsequently, phase conjugation mirrors were used to pass light through thick tissue [12] and finally, a direct inversion scheme using a measurement of the transfer matrix has also been demonstrated [15, 16]. Given this control over the spatial properties of the light field, several problems in diffusive transport have been studied, such as perfect focusing [17, 18], transmission in random media [19] and random matrix theory [15].

Given these developments, we have recently used wave-front shaping to demonstrate imaging behind turbid layers [7], where the interference based focus was scanned across a sample using the optical memory effect [20–22]. This principle has also been shown to work using phase conjugation as a means to create the initial focus. In both of these cases, the scanning works by a tilting of the incoming illumination, which leads to an additional linear phase shift [8]. This phase shift remains correlated during the scattering process over a certain length scale, which then leads to a corresponding shift in the position of the interference focus. This remaining correlation constitutes the optical memory effect, which has been discussed theoretically already in the late 1980's [20–22]. However, in the way this was implemented, the imaging is restricted to a single focal plane, which is very hindering for applications. In such applications, the creation of a focus behind a turbid layer relies on a beacon that delivers a contrast that can be detected an increased by wave-front shaping or phase conjugation. This can be a fluorescent particle [23] or a second harmonic generating quantum dot [8]. Thus, by being limited to a single plane of imaging, any interesting structures in the vicinity of the beacon but in a different plane cannot be imaged. Similar to two-photon microscopy, one would therefore like to be able to also investigate the third dimension. Unfortunately it is not possible to simply scan the sample for this purpose, since this will lead to random phase shifts induced by the scattering layer, which destroy the interference based focus. This will already happen for movements on a scale of the wavelength divided by the number of scattering events, i.e. a few nm in our case.

Here, we show that this can however be achieved by adding an additional parabolic phase shift to the spatial light modulation. This phase field works as the addition of a lens, which will move the focus in the z-direction. As with the linear phase shift for the planar scanning, the memory effects leads to a conservation of the change in focus over a certain angular range given by the thickness of the turbid layer. For a geometry as we are using, with a turbid layer some distance in front of the interesting structure, the range of scanning possible in the z-direction actually is bigger than that in the plane, as we will discuss below.

In the following, we will discuss first the setup and samples used to show that three dimensional imaging behind turbid layers is possible. Then we will discuss the theory of the memory effect and discuss the difference between planar and z-direction scanning, especially in the light of applications. Finally, we will show the results of our scanning microscope experiment before putting the technique in perspective in terms of its strengths and weaknesses in the conclusions.

2. Setup and samples

As a means to create samples illustrating the technique of fluorescent imaging behind a turbid layer, we covered one side of a glass microscope slide (thickness: $a = 1mm$) with Zinc Oxide pigment. The thickness of this layer was approximately 15 μm corresponding to more than 15 mean free paths. Thus, the light behind this layer is highly disordered and has undergone at least 200 scattering events. Thus, the layer is completely intransparent. On the other side of the microscope slide, we have attached a number of fluorescent nano-beads (Poybeads 450 nm), which can act as a marker. The absorption spectrum of the beads has a maximum around 480 nm, which corresponds to our illuminating light and emission maximally at 530 nm. The beads have a diameter of 450 nm comparable to the resolution we have previously determined in the x-y directions [7].

#159649 - $15.00 USD Received 7 Dec 2011; revised 23 Jan 2012; accepted 26 Jan 2012; published 31 Jan 2012
(C) 2012 OSA

The optical setup (see Fig. 1) consists of an illuminating blue laser (Spectra- Physics Cyan 40 mW, 488 nm), which is expanded and passed through a galvo-scanner (General Scanning LDS-07-OH) before being reflected off a spatial light modulator (Holoeye HEO 1080 P), which is computer controlled. The optimization of the incoming wave-front will be carried out by this SLM. The scanning in the x-y plane is carried out by the galvo scanner tilting the incoming wave front, whereas the z-direction will be scanned by the SLM by the addition of a parabolic phase pattern to the optimized one. The surface of the SLM is then imaged onto the surface of the scattering layer with a 40x microscope objective (Zeiss A-Plan 40x/0.25). This yields a illuminated spot on the turbid layer with a diameter of $r = 80\mu m$. Behind the sample, a Semrock GFP-3035B filter is used to discard the illuminating light, such that only the fluorescent signal is detected by a Photomultiplier (Hamamatsu). The signal in the photomultiplier is the scanned signal illustrated in the figures below after having passed through a low pass filter to increase the signal to noise ratio.

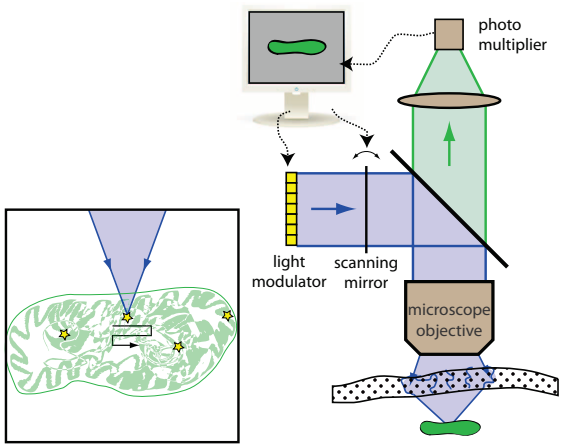

Fig. 1. Schematic setup of the experiment. The illuminating laser is expanded and reflected from the SLM shown in the figure. The SLM is imaged onto the surface of the turbid layer. In between, the light passes a scanning mirror, which adds a linear phase shift onto the light, which is used for scanning the focus in the $x-y$ plane. The sample consists of a turbid layer of ZnO pigment 15 μm thick on a glass cover slide of a thickness of 1 mm. On the other side of the glass slide, fluorescent latex beads of a diameter of 450 nm are placed. This mimics the situation in a natural sample, where a turbid shell hides a structure of interest, which has been labelled fluorescently (see inset). The fluorescent light is captured by a photomultiplier (PM) behind a fluorescent filter.

3. Theoretical description

As we have discussed previously, the memory effect leads to a retention of correlation of the phase over an angular scale determined by the thickness of the turbid medium. This is because the light transport through the turbid medium is confined to a cone with a width corresponding to the thickness of the medium. This is for a point illumination. When considering different channels through the turbid medium as illuminated by different point sources, then a change of the incoming phase remains correlated within this cone. Thus, phase changes of the order of $qL \simeq 1$ remain conserved, where $q = \theta k$ is the overall scattering vector with $k = 2\pi/\lambda$ and L is the thickness of the layer [20–22]. In the application for a scanning microscope, the angle

#159649 - $15.00 USD Received 7 Dec 2011; revised 23 Jan 2012; accepted 26 Jan 2012; published 31 Jan 2012
(C) 2012 OSA

θ corresponds to the angle covering the field of view of the microscope. For the experiments presented here with a layer of thickness $L = 15\mu m$ and a wavelength of $\lambda = 488nm$, this angle is $\theta \simeq 5 \cdot 10^{-3}$.

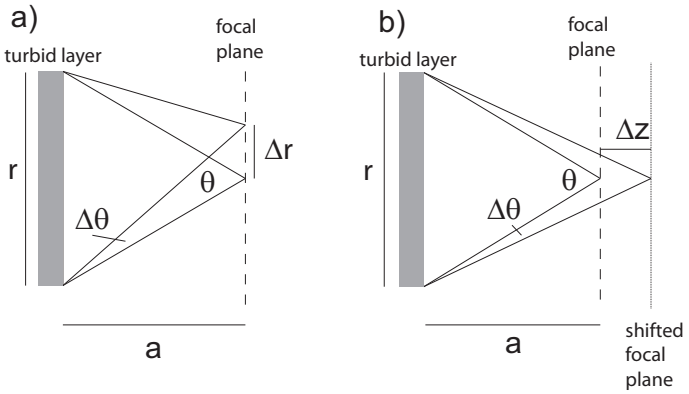

Fig. 2. Geometry of scanning in the different directions. The change in angle is limited by the memory effect. a) shows the situation for two-dimensional scanning in the $x-y$ plane. The change in angle here is given by $\Delta\theta = \Delta r/a$. In the z-direction in contrast, the change in angle is given by $\Delta\theta = r\Delta z/a^2$.

For two dimensional scanning in the $x-y$ plane, the angle determines directly the field of view together with the distance from the scattering layer a via $\Delta r = a\Delta\theta$. Thus, for a shift in the focal position, the phase of the incoming light must be changed by an amount corresponding to $\phi = kr \cdot \frac{\Delta r}{a}$. This change in phase is achieved by a tilting of the wave front by the galvo-scanner discussed above. In the geometry of our experiment, the intensity of the focus is halved over a distance of $\Delta r_{max} \simeq 5\mu m$, thus indicating the spatial resolution. For scanning in the z direction, the situation is slightly different, as illustrated in Fig. 2. The angle change now not only depends on the distance a, but also on the radial component. The shift in position is now given by $\Delta z = a^2\Delta\theta/r$, where the memory effect still correlates paths within the cone of angle $\theta \simeq 1/(kL)$. Again, this corresponds to a phase change of the incoming light of $\phi = kr^2 \cdot \frac{\Delta z}{a^2}$. This change in phase is obtained by adding a curvature to the incoming light field by adding a parabolic shift to the SLM, where the radius of curvature, R, corresponds to $1/R = \frac{\Delta z}{a^2}$. Again, for the geometry of the experiment described here, this yields a scanning range of $\Delta z_{max} \simeq 60\mu m$. Thus, for this geometry, the field of view obtained in the z-direction can be increased with respect to that in the $x-y$ plane. This is true as long as the size of the illumination is smaller than the distance of the structure of interest from the scattering layer. However, this difference also leads to an anisotropy in the size of the focal spot. In the z-direction, the focal spot will be larger by a factor of a/r as compared to the $x-y$ direction. This is because of the difference in path lengths in the different directions causing the interference based focus. With the geometry described above, we expect a resolution in the $x-y$ plane given by half the wavelength of the light used, i.e. 250 nm and a resolution in the z-direction of $3\mu m$.

With these two types of scanning, it is now possible to move the interference based focus, obtained by wave-front shaping, in all three directions of space. The field of view obtained with this technique determined by the memory effect is of sufficient size to be of interest in biological applications.

#159649 - $15.00 USD Received 7 Dec 2011; revised 23 Jan 2012; accepted 26 Jan 2012; published 31 Jan 2012
(C) 2012 OSA

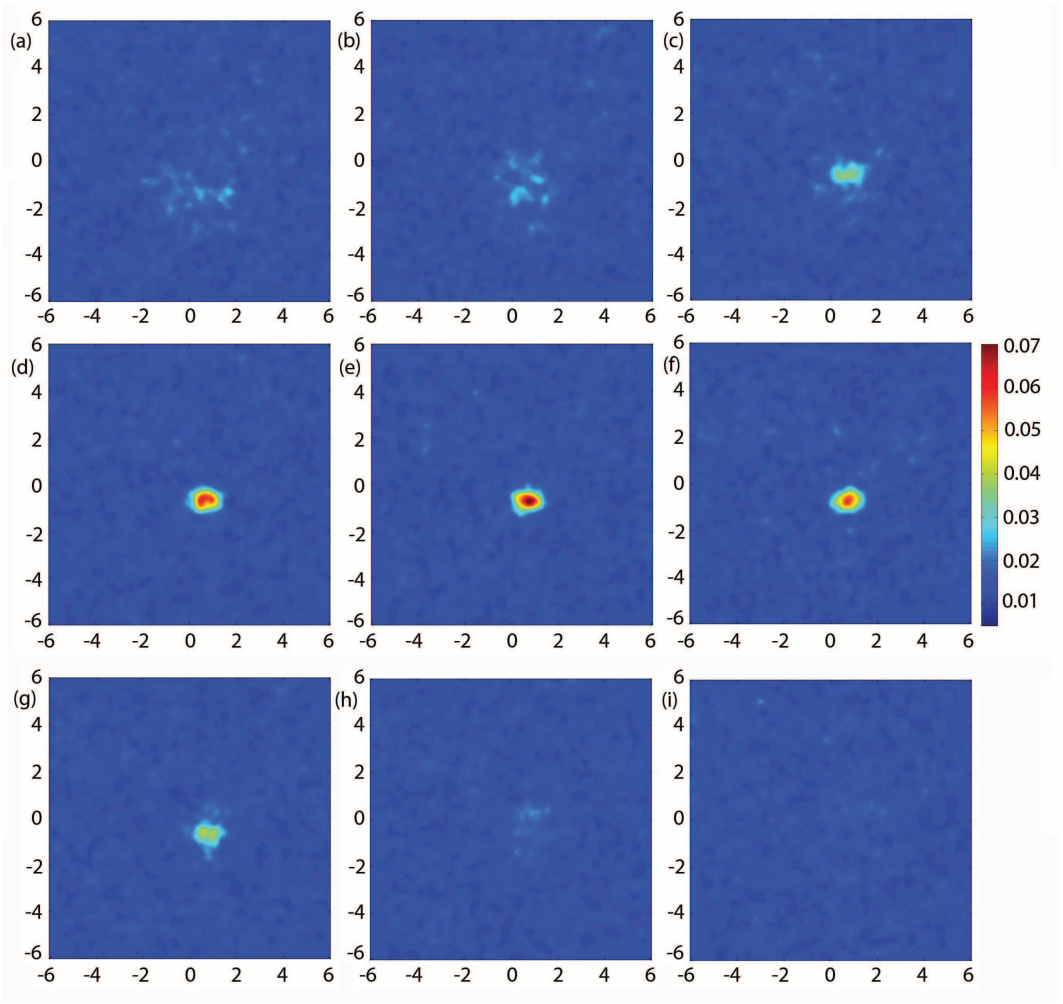

Fig. 3. (a)-(i) The fluorescence signal of a 450 nm diameter fluorescent bead hidden behind a turbid layer. The images show the scattered light fluorescence image of the same bead and on the same intensity scale, while the position of the focal plane differs for the images. In (a), the position is at -7 μm behind the bead and consecutively moves forward in steps of 2μm, until it lies 7 μm in front of the bead position in image (i). The center of the bead, which would therefore lie between image (d) and its neighbor has been added as well in part (e). Thus, the difference in z position between parts (d) and (e) as well as (e) and (f) corresponds to only 1 micron. The scan range in this case is a window in the $x-y$ plane of 12x12 μm^2. The three dimensional structure of the bead can be clearly seen.

#159649 - $15.00 USD Received 7 Dec 2011; revised 23 Jan 2012; accepted 26 Jan 2012; published 31 Jan 2012
(C) 2012 OSA

4. Experimental results

In Fig. 3, we show the fluorescence image of a 450 nm diameter bead hidden behind a turbid layer. The in-plane image has a resolution of 300 nm, as we have shown before [7], thus showing the size of the beads (see part (e)) of the figure, where the bead is fully in focus). The subsequent part of the figure show successive scan images of the same particle using a wave-front shaped focus, i.e. behind the turbid layer. The images are made at different nominal positions of the focal point, where the imaging plane is shifted in the z direction by 2 μm in every step, except between part (d) and (e) as well as (e) and (f), where the step size is one micron. The scanning through the bead can be clearly seen and a cut through the z-direction at the bead position yields the resolution that is obtained in this way. As discussed above, the scan range of the image is limited by the correlation length implied by the memory effect. The size of the image in the plane reflects the maximum scanning range, where the intensity in the focus has decreased by a factor of 2. This implies that a fluorescent bead at the edge of the image would be less intense by roughly a factor of 2 than one in the centre. In the z-direction, the scan range shown in Fig. 3 is much smaller than the theoretical limit, such that effectively the intensity in the focus is constant for all images.

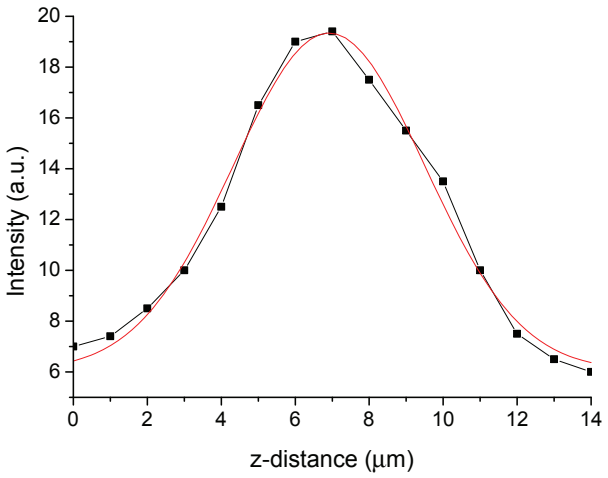

Fig. 4. The point spread function of the scattered light fluorescence microscope in the z-direction. The figure shows the intensity at the position of a fluorescent bead as a function of scanning depth. In contrast to Fig. 3, we show the full scanning range with a step size in the z-direction of 1 μm, giving a better measure of the depth resolution. This shows that the resolution in the z-direction is about 3 μm half width at half maximum, which is somewhat worse than in the $x-y$ plane thus showing that the interference focus is asymmetric. The red line shows a Gaussian fit with a standard deviation of 2.6(1) μm.

The resolution in the z-direction is presumably somewhat lower than in the $x-y$ plane, as can be seen from the bigger scanning range discussed above and the corresponding smaller adjustment in the phase shift for the same shift of the focus. This is shown in Fig. 4, where we show the fluorescent intensity at the position of the bead as a function of scanning depth. The resolution turns out to be 3.0(1) μm as measured by the half width at half maximum. This reduction in resolution however goes together with an increase in scanning range in the z-direction as discussed above.

#159649 - $15.00 USD Received 7 Dec 2011; revised 23 Jan 2012; accepted 26 Jan 2012; published 31 Jan 2012
(C) 2012 OSA

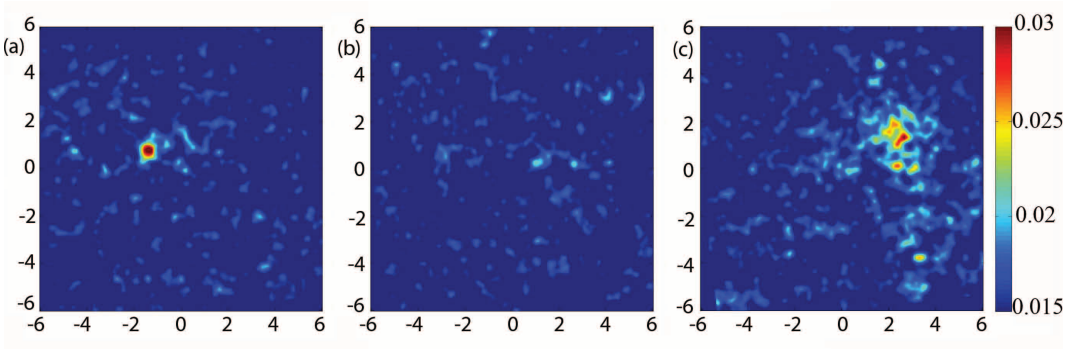

Fig. 5. (a)-(c) The fluorescence signal of two 450 nm diameter fluorescent beads hidden behind a turbid layer. The two beads are 55 μm apart in the z-direction and are at positions (-2,-1) and (2,-2) respectively in the (x,y) plane. The images show the scattered light fluorescence image on the same intensity scale, at three different depth. In (a), the position is at the first bead, whereas at (b) the position is 30 μm towards the second particle. Figure (c) finally is at a z position of 55 μm corresponding to the position of the second particle. The scan range in this case is a window in the $x-y$ plane of 12x12 μm^2. As discussed in the text, the z scan-range is 60 μm explaining the deteriorating quality of the image of the second particle. However, the three dimensional structure of the beads' positioning can be clearly seen.

In order to test the scanning range implied by the theoretical consideration above, we have also carried out an experiment with two fluorescent beads that have been hidden behind the same turbid screen, but where the second particle was shifted in the z-direction by a spacer of 55 μm. This corresponds to the scan range implied by the memory effect for our geometry, such that an image should still be possible at this distance however with worse quality. The change in phase incurred over that distance leads to a deterioration of the focus by roughly a factor of two with a corresponding change in resolution. The results of this are shown in Fig. 5, where the first particle (in the plane of the initial focus) is shown in part (a), an intermediate (x,y)-scan is shown for z=30 μm in part (b) and finally the second particle is shown in part (c) at a position of z = 55 μm. While clearly a particle can be seen in Fig. 5(c), the resolution is worse than that shown in Fig. 5(a) because of the limitations in scan range implied by the memory effect. The distance in the z covered by the scanning corresponds well to that of the theoretical expectation.

5. Conclusion

In conclusion, we have shown that scattered light fluorescence microscopy can be used for a three dimensional imaging of fluorescent structures hidden behind extremely turbid layers. The resolution of the images is limited by the size of the interference based focus, which in turn is limited by the wavelength of the light used. However, it is neither determined by the optical elements used in the setup nor the scattering properties of the layer in front of the structure of interest. The field of view available to the microscope is dependent on the distance to the turbid layer, as well as the thickness of the layer. We have previously shown that in an egg geometry, similar to our artificial samples, a plane of 12x12 μm^2 can be imaged [7]. In the z-direction, we have shown here that similar fields of view can be achieved. In fact, due to the way in which the distance between the layer and the structure of interest enters in the memory effect, the theoretically achievable field of view in the z-direction is actually bigger, in the case here up to 60 μm. Therefore, even structures close to the scattering layer could be studied in this way.

With this possibility of three dimensional scanning of the focus, applications of scattered

#159649 - $15.00 USD Received 7 Dec 2011; revised 23 Jan 2012; accepted 26 Jan 2012; published 31 Jan 2012
(C) 2012 OSA

light fluorescence microscopy become possible. This can work in the absence of any direct optical access, as long as there is e.g. a fluorescent structure on which the optimization can be carried out [23]. The main drawback of the technique remains in the temporal resolution, which is driven by the rate of change possible in the SLM used for the optimization. Currently this leads to long exposure times of the order of 30 minutes needed for creating three dimensional images. However, recent progress in the development of piezo-element based SLMs [24] make it possible to increase the speed of the SLM by at least three orders of magnitude [25], which makes applications possible. This can be seen by the time scale of the dynamics of fluctuations in e.g. Drosophila pupae, which is of the order of a minute [27]. Alternatively, phase conjugation may also allow an increase in temporal resolution [26].

Acknowledgments

This work was supported by the Swiss National Science Foundation as well as SystemsX.ch within the framework of the wingX RTD. One of us (GG) is grateful to Hans Bebie for helpful discussions.

#159649 - $15.00 USD Received 7 Dec 2011; revised 23 Jan 2012; accepted 26 Jan 2012; published 31 Jan 2012
(C) 2012 OSA